Eur. Phys. J. B **6**, 307–312 (1998)

THE EUROPEAN PHYSICAL JOURNAL B

New considerations on the role of covalency in ferroelectric niobates and tantalates

A. Villesuzanne[a], C. Elissalde, M. Pouchard, and J. Ravez

Institut de Chimie de la Matière Condensée de Bordeaux (ICMCB-CNRS), avenue du Dr. A. Schweitzer, 33608 Pessac, France

Received: 11 March 1998 / Revised: 22 June 1998 / Accepted: 16 July 1998

Abstract. Values of Curie temperature, T_C, and microwave relaxation frequency, f_r, of ferroelectric niobates and tantalates are found to be closely related to the metal-oxygen network covalency. Correlations previously evidenced in perovskite-type relaxors (PSN, PST) are confirmed here for $K(Ta_{1-x}Nb_x)O_3$ (KTN) compositions. The investigated physical characteristics, T_C and f_r, are determined *via* dielectric measurements performed in a wide frequency range (10^2–10^9 Hz) and as a function of temperature (250–800 K). On a theoretical point of view, bond covalencies are evaluated through tight-binding band structure calculations. The complex role of covalency on the metal potential is precised. Two antagonist effects acting on both the short-range interatomic repulsions and the rigidity and stability of the oxygen-metal network are discussed. The validity of this approach is comforted through the example of the oxyfluoride $K_3Li_{1.5}Ta_5O_{14.5}F_{0.5}$.

PACS. 71.20.-b Electron density of states and band structure of crystalline solids – 77.80.-e Ferroelectricity and antiferroelectricity – 77.84.Dy Niobates, titanates, tantalates, PZT ceramics, etc.

1 Introduction

Ferroelectric materials are of interest for various applications with regards to their high permittivities and their strong piezoelectric, pyroelectric, electrooptic and nonlinear optic coefficients. Their Curie temperature, T_C, was previously related to chemical bonding especially in corner-linked octahedron structure phases [1,2]. Various parameters were taken into account: steric, charge, covalency, electronic configuration, Jahn-Teller effects. Such chemical bonding – Curie temperature relations are of interest for prediction of new compositions adapted to a definite application. Depending on the type of application, low or high Curie temperature are required, *e.g.* T_C close to room temperature for dielectric, pyroelectric, electrooptic devices; on the contrary value of T_C much higher than room temperature for piezoelectric or nonlinear optic ones.

The present work deals with a theoretical approach of niobates and tantalates; in fact, such compositions are already very attractive for applications: $LiNbO_3$, $Ba_2NaNb_5O_{15}$ (optical parametric oscillators), $LiTaO_3$, (Ba, Sr)Nb_2O_6 (infrared detectors), $Pb(Mg_{1/3}Nb_{2/3})O_3$ (capacitors and actuators), $LiNbO_3$ (electromechanical transducers), $KNbO_3$, $LiNbO_3$ (holography), ... [3,4]. The Extended Hückel method coupled with the correlation chain model [5] was already used in a previous paper [6] to investigate the chemical bonding in $Pb(M_{1/2}M'_{1/2})O_3$ relaxor type ceramics (M = Sc, In ; M' = Nb, Ta). As a result, relations between microwave relaxation frequency, f_r ($10^8 < f_r < 10^9$ Hz), and covalency have been evidenced.

This approach is applied here to $K(Ta_{1-x}Nb_x)O_3$ (KTN) ceramics and extended to the role of covalency on T_C. The KTN solid solution was selected in order to avoid the problem of the complex influence of lead on the paraelectric-ferroelectric transition [7].

From a fundamental point of view, the aim of this study is a better understanding of the role of covalency on ferroelectricity in inorganic compounds. Previous works in this field generally conclude that covalency is necessary to soften the short-range interatomic repulsions opposed to the ferroelectric distortion [7–11]. A more complete view is proposed in this paper. This type of knowledge is also useful for phenomenological approaches, in which covalency acts on effective quantities as the oxygen ion polarizability [12].

2 Chemical bonding: theoretical approach

In order to investigate the chemical bonding in the KTN series, band structure calculations were performed by the Extended Hückel Tight-Binding method (EHTB) [13–15]. This method was chosen because it allows the computation of:

– overlap populations, which give a quantitative estimate of covalency,

[a] e-mail: ville@chimsol.icmcb.u-bordeaux.fr

– electron density maps, useful to visualize differences in chemical bonding between parent compounds.

Our study was focused on the evolution of the metal–oxygen network covalency in the KTN series, in order to seek for correlations with the T_C and f_r evolutions. Here covalency means the amount of mixing of oxygen $2p$ and metal d orbitals to form valence bands; it is evaluated quantitatively through the computation of the crystal orbital overlap population (COOP) [16,17] which is the extension of the Mulliken overlap population [18] to the periodic solid. For a given bond, the COOP is proportional to two quantities closely related to covalency: the overlap of atomic orbitals and the product of the associated LCAO coefficients, for every occupied crystal orbital. Although the COOP is the best suited, other quantities in the electronic structure are related to the metal–oxygen covalency: band widths, band gaps, electron population of metal d orbitals (formally 0 in ferroelectric oxides).

The EHTB method, because it uses the complete structural and chemical information (*i.e.* atomic orbitals and their overlap), is particularly well adapted to the study of chemical bonding, in relation with crystal structure, competing bonds, translation symmetry effects [19–23]. It gives quantitative informations on those electronic properties governed by the topology and nature of chemical bonding. It is a semiempirical method, but it uses only a few parameters; to each atomic orbital in the basis is attached an energy H_{ii} (diagonal element of the Hamiltonian matrix, related to electronegativity) and a Slater-type analytic expression: $\chi_{nlm}(r,\theta,\varphi) = Nr^{n-1}e^{-\zeta r/a_0}Y_{lm}(\theta,\varphi)$, where N is a normalization factor, a_0 is the Bohr radius, Y_{lm} is a spherical harmonic, n, l, m are the principal, orbital and magnetic quantum numbers, respectively. The ζ parameter is determined in order to reproduce the hydrogenlike orbital radial extension. In general, double-ζ expressions (linear combination of two Slater-type orbitals) are used for d orbitals.

The band structure and the mean metal–oxygen COOP for $K(Ta_{1-x}Nb_x)O_3$ were calculated for $x = 0$, 1/8, 1/4, 3/8, 1/2, 5/8, 3/4, 7/8, 1, in the cubic structure with metal–oxygen distances set to 1.99 Å (Ta–O and Nb–O bonds have the same lengths in $KTaO_3$ and $KNbO_3$). A 84 k-points grid was used to represent the irreducible Brillouin zone. The program EHMACC (n° 571 of the Quantum Chemistry Program Exchange) was used for the calculations. The EHTB parameters, tabulated in the EHMACC program, are given in Table 1.

It can be seen in Table 1 that the same energy is used for Ta $5d$ and Nb $4d$ atomic orbitals, while a 0.5 eV higher binding energy for Nb relative to Ta d orbitals is evoked by some authors [10]. Nethertheless, the use of an other EHTB parameters set [24] involving, among others, H_{ii} parameters of −10.001 and −9.569 eV for Nb $4d$ and Ta $5d$ orbitals, respectively, led us to the same conclusions. The EHTB method is here a semiempirical tool used to evaluate covalency; our conclusions, to be predictive in nature, have to be independent of the method of calculation.

Table 1. Extended Hückel parameters: atomic orbital energies and Slater-type exponents and ζ coefficients. Double-ζ expansions are used for d orbitals.

Element	Orbital	H_{ii} (eV)	ζ_i (c_i)
Ta	$5d$	−12.10	4.76 (0.6597)
			1.94 (0.5589)
	$6s$	−10.10	2.280
	$6p$	−6.86	2.241
Nb	$4d$	−12.10	4.08 (0.6401)
			1.64 (0.5516)
	$5s$	−10.10	1.890
	$5p$	−6.86	1.850
O	$2s$	−32.30	2.275
	$2p$	−14.80	2.275
K	$4s$	−4.34	1.000
	$4p$	−2.73	1.000

Table 2. Optimized sintering parameters for $K(Ta_{1-x}Nb_x)O_3$ compositions ($x = 0.3$, 0.4, 0.5, 0.7, 1).

x	$T_{sint.}$ (°C)	$\theta_{sint.}$ (min)	Additive	Compactn. (%)	Ref.
0.3	1120	60	LiF	91	[25]
0.4	1105	150	LiF	96	[25]
0.5	1105	240	Li_2CO_3	96	[26]
0.7	1040	150	LiF	96	[27]
1	990	60	LiF	92	[26]

To check for this, our results were confronted with first-principles calculations and experimental data on $KTaO_3$ and $KNbO_3$ (see discussion).

3 Experiments

Ceramics with composition $K(Ta_{1-x}Nb_x)O_3$ were prepared by solid state reaction from starting components K_2CO_3, Ta_2O_5 and Nb_2O_5. The optimized thermal treatments are summarized in Table 2.

In addition, an oxyfluoride ceramic with composition $K_3Li_{1.5}Ta_5O_{14.5}F_{0.5}$ was prepared by solid state reaction:

$$3KTaO_3 + LiTaO_3 + 0.5LiF + 0.5Ta_2O_5 \rightarrow K_3Li_{1.5}Ta_5O_{14.5}F_{0.5}.$$

After mixing and grinding the starting components in a dry box, the powder was pressed into disks and then calcined at 1150 °C for 15 h, in a platinum tube sealed under dry oxygen. The oxyfluoride was then sintered at 1300 °C for 4 h in the same conditions. X-ray diffraction study at 300 K showed a single phase of tetragonal tungsten bronze type.

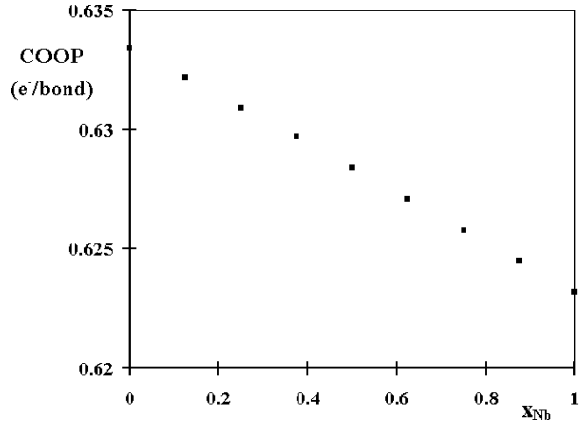

Fig. 1. Metal–oxygen mean COOP as a function of x in $K(Ta_{1-x}Nb_x)O_3$.

4 Results

In a previous study, the comparison of $Pb(Sc_{1/2}Ta_{1/2})O_3$ (PST) and $Pb(Sc_{1/2}Nb_{1/2})O_3$ (PSN) showed a correlation between the higher covalency in PST and the higher f_r values observed in this relaxor [6]. This correlation was interpreted as due to the stiffening of the structure (stronger Ta–O bonds relative to Nb–O ones), leading to higher f_r values.

4.1 $K(Ta_{1-x}Nb_x)O_3$: EHTB calculations

Figure 1 shows the evolution of the calculated mean metal–oxygen COOP as a function of x in $K(Ta_{1-x}Nb_x)O_3$. The COOP, that is, the covalency of the metal–oxygen network, decreases linearly from $KTaO_3$ to $KNbO_3$. The same result concerning Ta–O bonds relative to Nb–O bonds was obtained in reference [6] in the case of PST and PSN; in this previous paper the COOP values were weaker due to the competition with very covalent Pb–O bonds.

The energies of Ta 5*d* and Nb 4*d* atomic orbitals are the same in EHTB parameters. The bond lengths are equal too, as found experimentally. The difference in COOP's occurs because of the larger radial extension of Ta 5*d* compared to Nb 4*d* orbitals, leading to a greater overlap with oxygen 2*p* orbitals. This overlap effect is still dominating when a 0.5 eV higher binding energy is assumed for Nb relative to Ta *d* orbitals.

The EHTB method allows the calculation of the valence bands contribution to the electron density. In Figure 2 the differences in electron density between $KTaO_3$ and $KNbO_3$ are plotted in the (001) and (110) planes, respectively. The excess of electron density for $KTaO_3$ is found both in the region of the metal–oxygen bonds – giving the COOP's evolution – and in the [111] direction, which is the direction of the ferroelectric displacements.

Our calculations led to valence band widths of 1.93 and 1.81 eV for $KTaO_3$ and $KNbO_3$, respectively, indicating too a higher covalency for Ta–O relative to Nb–O bonds. The same tendency is found in first-principles calculations and by photoelectron spectroscopy; larger band widths are found then (5 to 6 eV theoretically [10,28,29]; 7 to 8 eV experimentally [29,30]). The underestimation of band widths in EHTB calculations is a common feature, like the large under- and overestimation of band gaps in density functional and Hartree-Fock *ab initio* approaches, respectively. We chose not to modify the EHTB parameters in order to fit band widths on other data, since our study is purely comparative in nature.

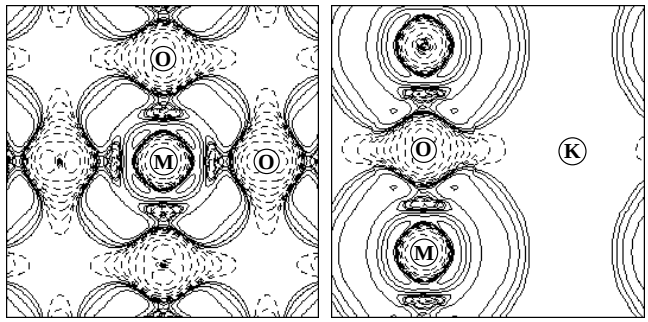

Fig. 2. Contour plots of the difference in valence electron density $\rho(KTaO_3)-\rho(KNbO_3)$. A logarithmic scale is used. Solid lines, positive values; dashed lines, negative values. M = Ta, Nb.

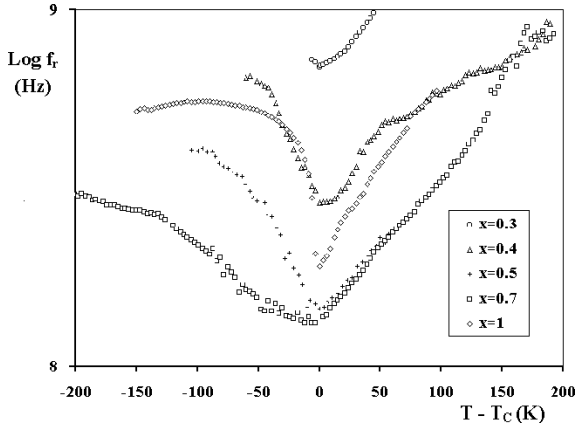

Fig. 3. Relaxation frequency as a function of $(T - T_C)$ for different compositions of the KTN system.

4.2 $K(Ta_{1-x}Nb_x)O_3$: dielectric measurements

The dielectric study of KTN ceramics in the concentration range $0.3 \leq x \leq 1$ was carried out between 10^6 and 10^9 Hz and as a function of temperature. The high frequency relaxation observed for each ceramic appears strongly dependent on both composition and temperature (Fig. 3). Whatever the Nb content, a minimum of f_r is observed close to T_C. The composition dependence of f_r shows clearly that a change of the relaxation mode is induced by the nature of the M–O bonds along the chain. As in the PST-PSN case, f_r (T_C) globally increases when the covalency of the metal–oxygen network increases. However, two regimes appear: f_r (T_C) seems to become

independent of covalency for $x > 0.5$. The mechanism of the dynamics evolution and the monotonical increase of T_C with x as the covalency decreases are discussed below.

5 Discussion

5.1 Covalency in KTN

Throughout our calculations Ta–O bonds were found more covalent than Nb–O bonds, for equal bond lengths in analogous compounds. This result is apparently opposite to what was argued in a previous paper [1], in which the role of covalency on T_C was discussed on the basis of Pauling electronegativity scale and on the comparison of $KNbO_3$ and $KTaO_3$.

A first point to discuss is the fact that covalency seems to be essential for the occurrence of ferroelectricity in inorganic compounds: the mixing of atomic orbitals allows to soften short-range repulsions which tend to cancel the ferroelectric distortion [7–11]. From this point of view, T_C should rise with covalency, and this behaviour is expected in significantly ionic compounds as titanates. Consequently, the argument on the role of covalency developed in reference [1] remains valid in many cases – *i.e.* highly ionic systems.

The second point is that covalency also plays a role on bond strength and on bulk energy. In the case of systems in which bonding bands are occupied by electrons and antibonding bands are empty, as in ferroelectric oxides (d^0 configuration for the metal), covalency may give strong bonds and an important stabilization of the bulk energy. In the case of significantly covalent systems, it has to be pointed here that this effect leads to a paraelectric phase of lower energy than the ferroelectric one. The paraelectric phase is stable enough, due to covalency, not to distort despite of the gain in electrostatic energy; moreover, the electrostatic component – *i.e.* interionic interactions – is expected to be largely lowered by the electron delocalization associated to covalency.

The fact that Ta^{5+}–O bonds are more covalent than Nb^{5+}–O bonds is due to a larger radial expansion of Ta $5d$ orbitals. This effect is not accounted for in electronegativity scales, which give an information on the energy difference between valence orbitals, not on their spatial overlap. Two arguments led to the opposite assumption of reference [1] concerning the covalency of Ta^{5+}–O and Nb^{5+}–O bonds: electronegativity considerations based on Pauling scale and the analogy with WO_3 and MoO_3, which have corner-sharing and edge-sharing octahedron structures, respectively. This indicates a lower charge carried by Mo, due to larger covalency. In the present paper, the explicit calculation of the electronic structure – COOP's in particular – give a larger covalency for Ta^{5+}–O bonds than for Nb^{5+}–O bonds. This result is retrieved in the Allred and Rochow scale [31] and in Zhang electronegativity scales for ions [32]. Maybe the most important point is that this covalency evolution from Ta to Nb is coherent with larger band widths obtained for $KTaO_3$ against $KNbO_3$ by both first-principles calculations [10,28,29] and photoelectron spectroscopy [29,30].

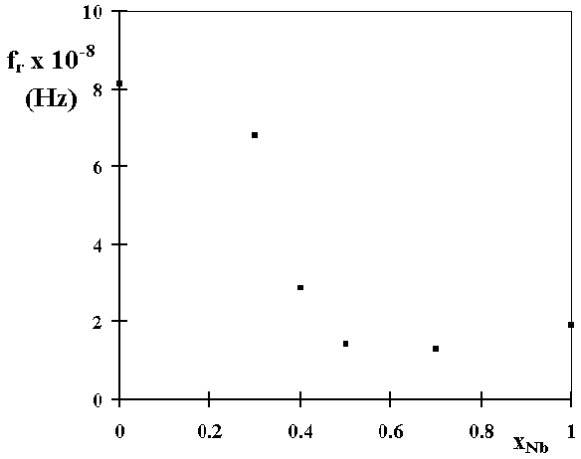

Fig. 4. Relaxation frequency at T_C as a function of x in $K(Ta_{1-x}Nb_x)O_3$.

5.2 f_r-chemical bonding relationships

Correlation between the microwave relaxation frequency and chemical bonding considerations have been evidenced and can be understood using the correlation chain model [5]. In this model, M ions are off-centered in their octahedral site and move in double-minimum potential with a barrier ΔE. Cooperative motion of ferroelectric active ions (Ta^{5+} and Nb^{5+}) along chains is considered. When x decreases in KTN, an increase of covalency influences the local environment and thus the shape of the potential. Stronger bonds are responsible, as a whole, for a "stiffening" of the network. The increase of f_r (T_C) observed experimentally is in agreement with such an assumption.

If the overall behaviour is consistent with an increase of f_r (T_C) with covalency, it is interesting to notice on Figure 4 that f_r (T_C) decreases first rapidly when x increases and then seems to stabilize from $x = 0.5$ to $x = 1$. In this regime, such an evolution can be interpreted on the basis of the large differences in the Ta and Nb potential slopes as a function of their displacement δ from the oxygen octahedron centre [28]. In the regime $x < 0.5$, there is a majority of non-harmonic flat potentials ($KTaO_3$-type); a weak decrease of the covalency is sufficient to bring about a strong fall of f_r. On increasing x, the system undergoes a transition to a regime ($x > 0.5$) with a majority of harmonic potentials with eight well-defined minima ($KNbO_3$-type) for which differences in covalency do not anymore influence significantly f_r (T_C), *i.e.* dynamics are no longer driven by the barrier height.

The proposed interpretation is that the decrease of the Nb content in KTN leads to a qualitative and quantitative crossover of the dynamics. For high Nb concentrations, the main contribution to the dielectric susceptibility is of relaxational type with relaxation frequencies lying below 10^9 Hz. When the Nb content is decreasing,

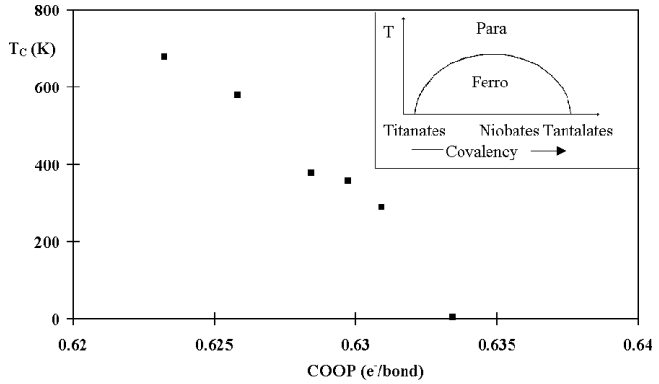

Fig. 5. T_C as a function of the metal–oxygen COOP in KTN and schematic phase diagram as a function of metal–oxygen covalency for d^0 transition metal perovskite oxides.

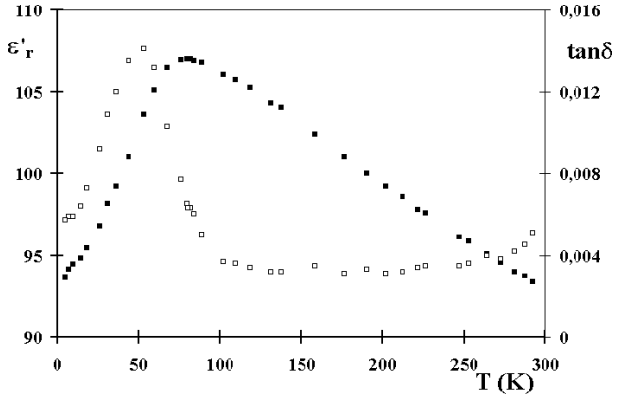

Fig. 6. Temperature dependence of ϵ'_r (■) and $\tan\delta$ (□) in $K_3Li_{1.5}Ta_5O_{14.5}F_{0.5}$.

this relaxation frequency gradually increases. The motion of relaxation along the chains, between the minima of a eight-well potential (hopping of large amplitude) shifts to phonon-like oscillations within one minimum. This is due to the progressive suppression of the interwell barriers by increasing covalency of the metal–oxygen bonds *i.e.* lower energy of the centered ion configuration. This evolution in the barriers may explain the potential slopes obtained by first-principles calculations for $KTaO_3$ and $KNbO_3$ as a function of the cell parameter [28].

5.3 T_C-chemical bonding relationships

Until now a softening role was attributed to covalency in the interplay between electrostatic energy and short-range repulsions for the occurrence of ferroelectricity in oxides. Although this description is satisfying for somewhat weakly covalent systems as $BaTiO_3$, it now appears that covalency may in turn, in more covalent systems as PST, PSN, KTN, inhibit the ferroelectric transition, by increasing the rigidity and the stability of the metal–oxygen network. This more complete view can be illustrated by the schematic phase diagram presented with the T_C evolution with COOP in KTN in Figure 5. The interest of such a diagram not only lies in a better understanding of ferroelectricity; it may allow to chemically tune dielectric characteristics in a compound series. Note that the T_C evolution with covalency observed in PSN (370 K) and PST (300 K) is in agreement with this phase diagram.

In order to confirm the underlined correlation between T_C and covalency, the effect of F–O substitution on a covalent tantalate compound was investigated. The selected compound is the tetragonal tungsten bronze-type ferroelectric $K_3Li_2Ta_5O_{15}$. The structure is completely filled and the solid solution $K_3Li_2(Ta_{1-x}Nb_x)_5O_{15}$ was already investigated [33]. The corresponding Curie temperature variation as a function of x shows a sharp increase from 7 K ($K_3Li_2Ta_5O_{15}$) to 753 K ($K_3Li_2Nb_5O_{15}$) when x increases [34]. As in KTN, a higher value of T_C is observed when the covalency within the octahedron site is reduced *i.e.* when tantalum is replaced by niobium. As fluorides are generally much more ionic than oxides, the F–O substitution in $K_3Li_2Ta_5O_{15}$ should act as the Nb–Ta one and then softens the crystalline network by reducing the covalency in the octahedra. As a result the value of T_C should increase, contrary to the usually expected evolution in an oxyfluoride.

The Curie temperature was determined by dielectric measurements performed from 5 to 300 K. The temperature dependencies of both ϵ'_r and loss tangent, $\tan\delta$, at low frequency (10^3 Hz) are represented in Figure 6. A maximum of ϵ'_r for a temperature close to 80 K was clearly observed both on cooling and on heating. This peak is associated with a minimum of $\tan\delta$ as it is usually observed in ferroelectric compounds. The Curie temperature of the oxyfluoride is then, here, higher than the one of the corresponding oxide ($T_C = 7$ K). This result can be explained here also on considering a softening of the network resulting from the decrease of the covalency within octahedral sites; the F–O substitution leads naturally to more ionic bonds. Moreover, the covalency effect appears to be more important on T_C than the decrease of electrostatic energy, which tends to lower T_C.

The results obtained here for this tantalate oxyfluoride is different from those obtained with more ionic compounds as for instance titanates or niobates: with both perovskites and tetragonal tungsten bronze structural types, the Curie temperature decreases strongly with the rate of F–O substitution whatever the necessary cationic substitution in order to respect the electric neutrality [35].

6 Conclusion

Correlations were evidenced between f_r, T_C and chemical bonding in niobate and tantalate ferroelectrics. This allowed a deeper insight on the role of covalency, which acts on the metal potential in two ways:

– As already known, it favours the ferroelectric distortion by softening the short-range interatomic repulsions. The corresponding effect on the metal potential slope is an increase of the eight-well depth.

– As shown in the present work, an increase of covalency may stiffen enough the metal–oxygen network to inhibit the ferroelectric distortion. Thus, it also contributes to reduce the barrier height, leading to the flat and anharmonic Ta potential slope in $KTaO_3$.

On a practical point of view, these two antagonist effects can be used, in a predictive way, to tune physical characteristics as transition temperature and microwave relaxation frequency *via* chemical parameters (substitutions, competing bonds, ...). This approach was successfully used to increase T_C in the ferroelectric $K_3Li_2Ta_5O_{15}$, by F^-–$(O^{2-} + Li^+)$ substitution. It has to be emphasized that the computation of COOP's appear to be the more precise way to evaluate bond covalency. Any approach based on electronegativity scales is dealing with bond ionicity, covalency being in this case just a measure of the departure from the purely ionic picture.

Work is in progress to extend this approach on niobates and tantalates to other ferroelectric compositions.

The authors acknowledge the "Pôle de Modélisation Numérique Intensive", Université de Bordeaux I, for computing facilities.

References

1. J. Ravez, M. Pouchard, P. Hagenmuller, Eur. J. Solid State Inorg. Chem. **25**, 1107 (1991).
2. M. Pouchard, J.P. Chaminade, A. Perron, J. Ravez, P. Hagenmuller, J. Solid State Chem. **14**, 274 (1975).
3. J. Ravez, F. Micheron, L'actualité Chimique **9** (1979).
4. Y. Xu, *Ferroelectric Materials and their applications*, (North-Holland, Amsterdam, 1991).
5. R. Comes, M. Lambert, A. Guinier, Solid State Commun. **6**, 715 (1968).
6. C. Elissalde, A. Villesuzanne, J. Ravez, M. Pouchard, Ferroelectrics **199**, 131 (1997).
7. R.E. Cohen, Nature **358**, 136 (1992).
8. R.E. Cohen, H. Krakauer, Phys. Rev. B **42**, 6416 (1990).
9. M. Posternak, R. Resta, A. Baldereschi, Phys. Rev. B **50**, 8911 (1994).
10. D.J. Singh, Phys. Rev. B **53**, 176 (1996).
11. G. Fabricius, E.L. Peltzer, C.O. Rodriguez, A.P. Ayala, P. de la Presa, A. Lopez Garcia, Phys. Rev. B **55**, 164 (1997).
12. M. Sepliarsky, M.G. Stachiotti, R.L. Migoni, Phys. Rev. B **52**, 4044 (1995).
13. R. Hoffmann, J. Chem. Phys. **39**, 1397 (1963).
14. J.H. Ammeter, H.B. Bürgi, J.C. Thibeault, R. Hoffmann, J. Am. Chem. Soc. **100**, 3686 (1978).
15. M.H. Whangbo, R. Hoffmann, J. Am. Chem. Soc. **100**, 6093 (1978).
16. T. Hughbanks, R. Hoffmann, J. Am. Chem. Soc. **105**, 3528 (1983).
17. R. Hoffmann, *Solids and Surfaces: A Chemist's View of Bonding in Extended Structures* (VCH, New York, 1988).
18. R.S. Mulliken, J. Chem. Phys. **23**, 1833 (1955).
19. J.K. Burdett, S.A. Gramsh, Inorg. Chem. **33**, 4309 (1994).
20. E. Canadell, M.H. Whangbo, Chem. Rev. **91**, 965 (1991).
21. J.K. Burdett, *Chemical Bonding in Solids* (Oxford University Press, New York, 1995).
22. A. Villesuzanne, M. Pouchard, C. R. Acad. Sci. Paris **310**, Série II, 155 (1996).
23. A. Simon, Angew. Chem. Int. Ed. Engl. **36**, 1788 (1997).
24. G.A. Landrum, YAeHMOP, Baker Laboratory, Cornell University, Ithaca, New York 14853-1301. `http://overlap.chem.cornell.edu.8080/yaehmop.html`.
25. H. Khemakhem, J. Ravez, A. Daoud, Ferroelectrics **188**, 41 (1996).
26. P. Dubernet, J. Ravez, A. Pigram, Phys. Stat. Sol. (a) **152**, 555 (1995).
27. H. Khemakhem, J. Ravez, P. Dubernet, A. Daoud, Phase Transition **56**, 199 (1996).
28. A.V. Postnikov, T. Neumann, G. Borstel, M. Methfessel, Phys. Rev. B **48**, 5910 (1993).
29. T. Neumann, G. Borstel, C. Scharfschwerdt, M. Neumann, Phys. Rev. B **46**, 10623 (1992).
30. A. Winiarski, T. Neumann, B. Mayer, G. Borstel, M. Neumann, Phys. State Sol. (b) **183**, 475 (1994).
31. E.J. Little Jr., M.M. Jones, J. Chem. Ed. **37**, 231 (1960).
32. Y. Zhang, Inorg. Chem. **21**, 3886 (1982).
33. T. Fukuda, Jpn J. Appl. Phys. **9**, 599 (1970).
34. T. Fukuda, H. Hirano, S. Koide, J. Crys. Growth **6**, 293 (1970).
35. S.C. Abrahams, J. Ravez, Ferroelectrics **135**, 21 (1992).